www.amlett.com, www.vbripress.com/aml, DOI: 10.5185/amlett.2015.5895 Published online by the VBRI Press in 2015

Synthesis and characterization of semi-interpenetrating polymer network based on single-walled carbon nanotubes

A. Jayakumar[1], N. Malarvizhi[1], B. Rajeswari[1], A. Murali[1], Debasis Samanta[1], P. Saravanan[2], C. Muralidharan[2], Sellamuthu N. Jaisankar[1*]

[1]*Polymer Division, Council of Scientific and Industrial Research (CSIR)-Central Leather Research Institute (CLRI), Adyar, Chennai 600020, India*
[2]*Leather Processing, Council of Scientific and Industrial Research (CSIR)-Central Leather Research Institute (CLRI), Adyar, Chennai 600020, India*

[*]Corresponding author. Tel: (+91) 44-24422059; E-mail: snjaio@yahoo.com; snjsankar@clri.res.in

Received: 09 March 2015, Revised: 28 April 2015 and Accepted: 14 June 2015

ABSTRACT

Semi-interpenetrating polymer networks (semi-IPNs) based polyurethane (PU), polyvinyl alcohol (PVA) and functionalized single–walled carbon nanotubes (*f*-SWCNTs), films were prepared using sequential polymerization technique. Carboxyl functionalized SWCNTs in semi-IPNs matrixes were confirmed by Raman spectroscopy and hydrogen bond interactions were studied using attenuated total reflectance fourier transform infrared spectroscopy. The soft segments of the PU with nanotubes interact much stronger than hard segments, this was observed by Differential Scanning Calorimeter. The activation energy and thermal degradation temperatures were calculated from thermogravimetric analysis. The tensile strength and Young's modulus was increases with increase *f*-SWCNTs loadings. The AFM micrographs clearly shows *f*-SWCNTs were located in semi-IPNs matrix. Further, SWCNTs are attached in PU and spherical structures were dispersed in polymer matrix. The surface activation energy of the composites were increases up to 29 kJ/mole with increasing SWCNTs content on PU networks. Copyright © 2015 VBRI Press.

Keywords: Nanocomposites; polyurethane; semi-IPNs; polyvinyl alcohol; SWCNTs.

Introduction

The multiuse materials of polyurethane (PU) used for coatings, adhesives, thermoplastic elastomer **[1]** nanofibers and thermosetting applications. The PU consists of soft and hard segments. The soft segment leads to high molecular weight polyether or polyester diols and hard segment which are composed of isocynates and lower molecular weight diols or diamines **[2-5].** By the addition of carbon nanotubes (CNTs) into polyurethane matrix, it could be enhances the thermal and mechanical properties **[6, 7].** Polyvinyl alcohol (PVA) is an environment friendly biodegradable polymer **[8].** It has individual attention as its good flexibility, high transparency, chemical resistance, hydrophilic properties and antielectrostatic properties. In PVA, free hydroxyl groups react with diisocynate to form a copolymers exhibit good mechanical stability and swelling properties with wide commercial applications **[9-19].** Semi-IPNs polymer composite materials are combined one or more network and linear or branched polymer characterized by molecular scale of penetration at least one of the polymer components is cross-linked and the other is linear. Interpenetrating polymer networks (IPNs) are consists of two or more different polymer networks can form a permanent entanglement with strong bond along with polymer network **[20-25].** Several methods can be used to synthesis IPNs by simultaneous, sequential and latex IPNs. IPNs possess more advantages in comparison of normal polymer blends. Normally IPNs results in multiphase morphology along the phase separation may be prohibited by stable interlocking of entangled. The IPNs material applications of are depend on the domain size, glass transition temperature (T_g), phase permanence and mixing of the component networks. Most of the IPNs pairs are immiscible due to improve the miscibility and degree of interpenetration of the constituents **[26-29]**. In this paper, we report the synthesis of semi-IPNs based polyurethane and trimethylol propane (TMP), polyethylene glycol (PEG), diisocynate, PVA in presence of COOH-SWCNTs using sequential polymerization technique.

Experimental

Materials

The polyethylene glycol (PEG) with (Mw ~1000), polyvinyl alcohol (PVA), isophoron diisocynate (IPDI, 98%), trimethylol propane (TMP) as a cross-link agent and

single-walled carbon nanotubes (SWCNTs) were used as received from Sigma Aldrich, USA. Dibutyltin dilaurate (DBTDL) used as a catalyst, tetrahydrofuran (THF) HPLC grade and anhydrous dimethyl formamide (DMF) used as the solvents were purchased from Aldrich, USA. Dimethyl sulphoxide (DMSO) was purchased from MERCK, India.

Preparation of carboxylic acid functionalized SWCNTs (COOH-SWCNTs)

100mg of pristine SWCNTs were suspended in nitric acid and sulphuric acid (3:1 v/v) in the ratio using ultra sonicator for 30 min. Then the mixture of SWCNTs solution was transferred to three necked RB flask fitted with condenser, reflux for 24 h at 90°C. The mixtures of CNTs solution was poured to 3 L of deionized water for neutralizing to the neutral pH and further the solution was filtered using 0.2 µm PTFE membranes, for removing impurities from SWCNTs. Finally all the solution was centrifuged at 10000 rpm and dried at 40°C under vacuum. The carboxyl functionalized SWCNTs confirmed by using Raman spectroscopy D band (1360 cm^{-1}), G band (1589 cm^{-1}) and FT-IR spectroscopy C=O (1636 cm^{-1}),OH (3426 cm^{-1}), and C-O (1244 cm^{-1}) **[30].**

Preparation of semi- IPNs based PU nanotube composites

2g of PVA and 1g of PEG were taken in a three necked reaction flask. A 1:1 ratio of equal amount of DMF and DMSO added to the PVA and PEG polymer mixture. The mixtures were dehydrated continuous by stirring at 60°C for 1h under N_2 atmosphere. Then 2g of IPDI and 0.001 wt % of DBTDL was slowly added with using additional funnel into PVA-PEG solution with constant stirring for 3h and raised the temperature at up to 75°C under nitrogen atmosphere. Subsequently 0.001, 0.005, 0.01, 0.05, and 0.1 (PUNT1, PUNT2, PUNT3, PUNT4 and PUNT5), weight percentage of carboxylic acid functionalized single-walled carbon nanotubes were dispersed in 1:1 ratio of organic solvent mixtures (DMF:DMSO) by using ultra sonication for 1h **(Table 1)**. 0.166 g of TMP was added to the mixture and stirred well at 75°C for 1h. Final solution was poured into preheated glass mould and curing at room temperature for 5h then kept in the oven for 15h at 60°C. After curing the sample of PU nanotube composites was used for further characterizations.

Characterization of semi-IPNs based on carbon nanotube composites (CNTs)

The IPNs based CNT composites were characterized by confocal Raman microscopy, nanophoton, Raman11, Japan and Attenuated total reflectance Fourier transform infrared spectroscopy (ATR-FTIR) ZASCOFTIR-4200, Canada. The spectra were collected from the range 4000 to 600 cm^{-1} at 25°C with a resolution of 3cm^{-1} by 40 scans. The CNTs are dispersed in organic solvent mixture, using probe sonicator Sonics VCX 750 750W, 20 KHz, 60 % amplitude, Sonics & Materials, Inc. Newtown, USA. The thermal properties of thermogravimetric analysis (TGA), the IPNs were characterized by TG Analysis Model Q50, TA instruments Waters Pvt. Ltd, Bangalore, India, with a heating rate of 10 ºC per min from 40 ºC to 700 ºC under nitrogen atmosphere. Differential scanning calorimetric (DSC) analysis was done using Model Q 200, TA instruments, at a heating rate 10ºC per min under N_2 atmosphere from -70ºC to 300ºC. The mechanical properties like tensile strength, Young's modulus and percentage elongation at break were measured using universal testing machine (Instron 3369, Instron, Norwood, MA, USA) at a cross- head speed of 50 mm per min with 0.1 mm of thickness, as per the ASTM D 635 method. The morphology analysis determined by using optical microscopy determined with an OLYMPUS BX 50 optical polarizing microscope. The photographs were taken using an OLYMPUS C7070 digital Sony camera. The surface morphology of IPNs based on the PU/PVA nanotube composites were analyzed using AFM (NTMDT, Netherland) model of NTEGRA PRIMA, cantilever of NSG10 and tip diameter 10 nm.

Results and discussion

The ATR-FTIR shows peak at (-C=O: 1728cm^{-1}, 3389cm^{-1}: -NH, 2923 cm^{-1}: -C-H, 1633 cm^{-1}: -CO-NH and 1541 cm^{-1}: C-N) were confirmed the formation of PU nanotube composites. Further repeat at 3412 cm^{-1} corresponds to carboxylic functionalized SWCNTs. The peak in the range of 2750-3012 cm^{-1} and 3037-3697 cm^{-1} are the characteristics of C-H and N-H stretching vibrations, respectively **[31-34]**. The urethane linkage of amide carbonyl group (C=O) to transmittance a lower frequencies. The peak at 1739 cm^{-1} was clearly indicated to carbonyl stretching vibration. The C-N amide stretching vibration peak at 1247 cm^{-1} **[35-39]**. There is no peak at 2275 cm^{-1} was confirmed that all the NCO is reacted and formed the polymer **[40-42].** The amide carbonyl group at 1739 cm^{-1} shifts with increased weight percentage of *f*-SWCNTs. The broad peak at 3389 cm^{-1} corresponds to presence of secondary amine in PU network as shown in **Fig. 1 [ESI]**. The expanded region of C=O and CH_2 FTIR spectrum as shown in **Fig. 1**.

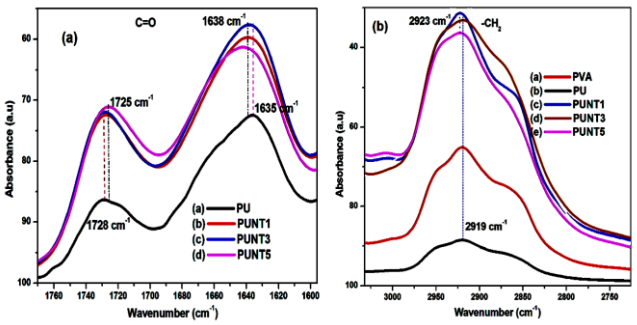

Fig. 1. ATR-FTIR spectra of expanded region from 3070 to 1600 cm^{-1} (a) C=O at 1770-1596 cm^{-1} and (b) -CH_2 at 3032 – 2726 cm^{-1}.

The nanotube composites were characterized by Raman spectroscopy to identify the disorder band and tangential band, radial breathing mode (RBM) of the nanotubes as well as the sp^3 to sp^2 hybridized carbon centers of nanotubes.

The RBM can be correlate to the tube diameter υ (cm^{-1}) = 223.75/d (nm) + Δ υ (cm^{-1}), which helps to calculated the diameter of the CNTs **[43].** The characteristic peaks of f-

SWCNTs observed at RBM: 168 cm^{-1}, D band: 1360.64 cm^{-1}, G band: 1589.36 cm^{-1} respectively, whereas the -N-H stretching vibration of amide I (1772 cm^{-1}), amide II (1539 cm^{-1}) and amide III (1324 cm^{-1}) with respect to amide urethane linkage was confirmed in PU nanotube composites. In addition, Raman spectroscopy clearly shows the formation of PU nanocomposites, *f*-SWCNTs could covalently attached to the polymer network as shown in **Fig. 2**.

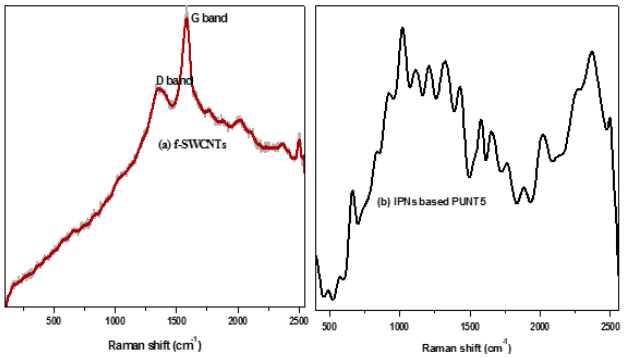

Fig. 2. Confocal Raman spectra of (a) *f*-SWCNTs and (b) PUNT5.

The stress-strain behaviour of semi-IPNs based PU nanotubes composite were measured and are presented in **Table 1.** Tensile strength and Young's modulus increases with increasing *f*-SWCNTs content, this may be due to the interaction and dispersion of functionalized SWCNTs in the PU nanotube matrix. All the IPNs (**Table 1**) show the improvement in modulus compare to the neat polymer **[44]**. The IPNs based PU nanotube composites were indicates that the PUNT5 exhibits high strength and modulus compared to the PU neat, this ratio may be the best ratio for coating applications.

Table 1. Stress–strain behaviour of semi-IPNs based PU and PUNT composites.

Codes	T.S (MPa)	Y.M (MPa)	E.B (%)	*f*-SWCNTs (Wt %)	S.T (mm)
PU	0.063	3.94	6.45	-	
PUNT1	0.084	4.79	1.77	0.001	
PUNT2	0.093	4.86	1.91	0.005	
PUNT3	0.180	5.14	4.64	0.010	0.1
PUNT4	0.242	9.91	0.65	0.050	
PUNT5	0.254	15.90	1.54	0.100	

T.S – Tensile Strength; Y.M – Young's Modulus; E.B – Elongation at Break; S.T – Sample Thickness.

Thermal stability of the polyurethane nanotube composite films was studied with TGA and DSC. **Fig. 2 [ESI]** shows thermal degradation temperature of semi-IPNs based polyurethane neat and polyurethane carbon nanotube composites. The PU neat and PU nanocomposites having two stage decomposition transition temperature. The maximum weight loss of the composite film was observed at 160°C and 460°C.

The first degradation step corresponding to the weight loss of bound water. The second step decomposition temperature was observed by organic compound remove. The polyurethane nanotubes composite main chain decomposes at 465 °C **[45].** The degradation of polymer has shown that the existences of *f*-SWCNTs in the polymer matrix prevents the thermal decomposition and improve the thermal stability of nanotube, this is due to the better interactions between PU and *f*-SWCNTs. **Table 2** shows that the neat PU and polyurethane nanotube composites degradation temperatures of $Tmax^1$ and $Tmax^2$ respectively.

Table 2. Thermal transition temperature of IPNs.

Sample codes	DSC		TGA		Residue (%) at 600 °C
	T_g (°C)	T_m (°C)	T_{max}^1 (°C)	T_{max}^2 (°C)	
PU	-65	109	64	100	10.21
PUNT1	-66	193	262	359	8.89
PUNT3	-67	157	265	349	6.37
PUNT5	-66	197	260	364	8.40

The two degradation temperatures are depends on hard and soft segments of polyurethane. The glass transition temperatures (T_g) and melting temperature (T_m) of PU neat and PU nanotube composites were studied by DSC and are depicted in **Fig. 3**. **Fig. 3** shows that the melting temperature T_m at 109, 157 and 197 °C of PU, PUNT3 and PUNT5 corresponding to the soft segments of PU matrix. The endothermic peak at 197 °C corresponds to PU nanotube composites incorporation of SWCNTs in PU matrix T_m was gradually increased due to uniform dispersion of *f*-SWCNTs into PU matrix. Thermogravimetric analysis by using kinetics of thermal degradation was investigated. Thermal degradation of PU and PU carbon nanotube composites were determined by the percentage weight loss against temperature. Several researchers analogous to the Kissinger method have been used to determine the activation energy from plots in logarithm of the heating rate versus the inverse of the temperature at maximum reaction rate experiments **[46].**

$$\ln (\beta/T^2max) = - Ea / RTmax + \{\ln AR/Ea + \ln [n (1-\alpha max) n-1]\} \quad - (1)$$

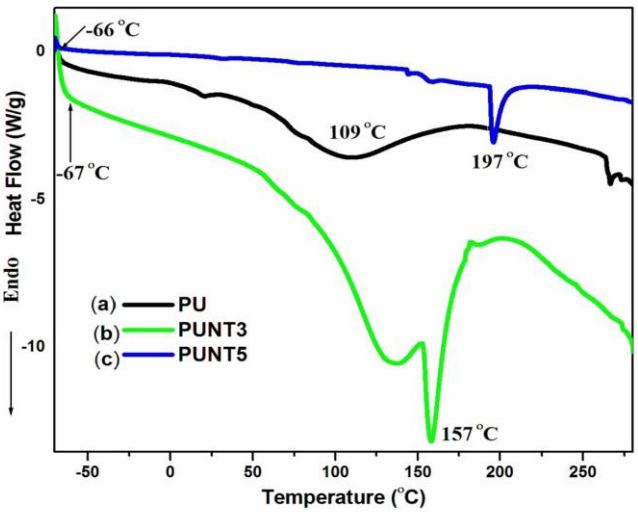

Fig. 3. Thermograms of Semi-IPNs based: (a) PU (b) PUNT3 and (c) PUNT5.

where, Tmax is the thermal degradation curves which corresponds to the maximum reaction rate; β is the heating rate; R is the ideal gas constant (8.314 J/(K mole); Ea is the

activation energy; A is the pre-exponential factor; αmax is the maximum conversion and n is the order of reaction. The activation energy calculated from the slope a plot of ln (β/T^2max) versus 1/Tmax, and fitting linear to a straight line. **Fig. 4** shows that the relationship given by above equation 1, known as Kissinger techniques. The surface activation energy of semi IPNs based nanotube composites were increased up to 7-29 kJ/mole as shown in table 3. The morphology of IPNs based PU and PU nanotube composites were identified the atomic force microscopy. The *f*-SWCNTs higher wt % in polyurethane matrix have some block spots agglomeration were observed. Several researchers observed that PU interconnects with *f*-SWCNTs agglomerated in polymer matrix. AFM can be used in two different kinds of mode contact and semi-contact (Tapping mode), these two modes also were performed in air. The contact mode and commercial Si cantilevers/ tips were used for all an AFM instruments. All through an AFM experiment the optimal condition (set point, scan size and scan speed) was adjusted to allow the better resolution of image, topographic (height) and phase image get simultaneously obtained **[47].** AFM sample preparation of 1 mg *f*-SWCNTs in 1ml DMF heating at 50ºC for 1 h and sonicated for approximately 4 min. PUNT5 composite solution was onto cleaned glass plates, kept into a vacuum oven at 45 ºC. The semi-IPNs were coated on 1 cm^2 of square glass plate surface. AFM image of semi-IPNs based PU network on coating of *f*-SWCNTs topography and phase image spherical shape of *f*-SWCNTs aggregated in PUNT5 composites by used semi contact mode. An OPM **Fig. 3** ESI and AFM image clearly shows that spherical types of structure (**Fig. 5**) were observed due to cross linked agent on polymer matrix **[48].**

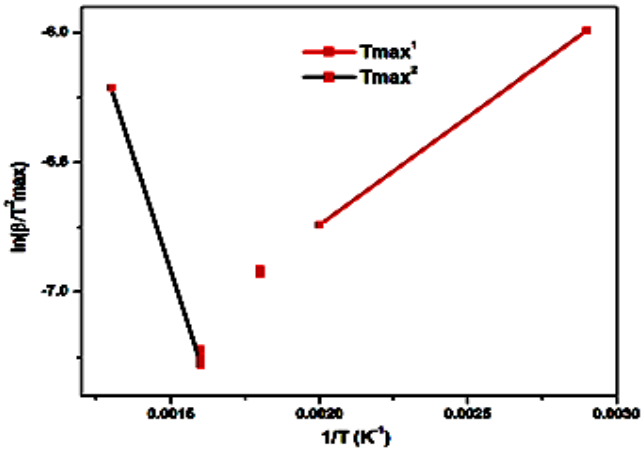

Fig. 4. The Kissinger pots of semi-IPNs.

Table 3. Activation energy and R^2 value of Semi-IPNs by using Kissinger method.

Samples code at degradation stages	Slope value	E_a (kJ/mole)	R^2
Semi-IPNs based PUNT composite at the (I) degradation stage	-8420	7.0	0.9997
Semi-IPNs based PUNT composite at the (II) degradation stage	-3483	29.0	0.9988

E_a – Activation energy; R^2 – Correlation coefficient.

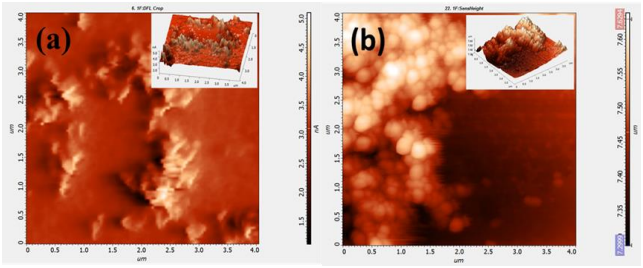

Fig. 5. Morphology of semi-IPNs based AFM (a) PU and (b) PUNT5.

Conclusion

In this work, we have successfully synthesized semi- IPNs based PU carbon nanotube composites by sequential polymerization method. The functionalized single-walled carbon nanotubes have better dispersion in polyurethane matrix. The thermal study proves the activation energy leading to high stability on semi-IPNs. The morphology studies of OPM and AFM shows in that microphase separated morphological structure and better mechanical properties. Further, this kind of semi-IPNs based nanotube composites could be used for coating application.

Acknowledgements
The authors acknowledge the funding from CSIR cross cluster project ZERIS (WP-21 CSC 0103).

Reference

1. Xiaoxiang, Z.; Songtao, H.; Meng, W.; Jia, Y.; Qasim, K.; Jintang, S.; Long, B.; *Nanotechnology*, **2015**, *26*, 115501. **DOI**:10.1088/0957-4484/26/11/115501
2. Murali, A.; Senthil, A. G. T.; Jaisankar, S. N.; Mandal, A. B.; *RSC Adv*., **2014**, *4*, 62947. **DOI**: 10.1039/C4RA07636B
3. Nimai, B.; Pratyay, B.; *J. Phys. Chem. C*, **2014**,*118*, 10640. **DOI**: 10.1021/jp501972u
4. Sawaryn, C.; Landfester, K.; Taden, A.; *Polymer*, **2011**, *52*, 3277. **DOI**:10.1016/j.polymer.2011.04.064
5. Xia, H.; Song, M.; *Soft Matter*, **2005**, *1*, 386. **DOI**: 10.1039/B509038E
6. Kim, C. I.; Lee, P. I.; *Pharm. Res.*, **1992**, *9*, 10. **DOI:** 10.1023/A:1018963223484
7. Wang, T.; Turhan, M.; Gunasekaran, S.; *Polym. Int.*, **2004**, *53*, 911. **DOI:** 10.1002/pi.1461
8. Wang, Z.; Luo, J. T.; Zhu, X. X.; Jin, S. J.; Tomaszewski, M.J.; *J. Comb. Chem.*, **2004**, *6*, 961. **DOI:** 10.1021/cc0499183
9. Wan, Y.; Huang, W.Q.; Wang, Z.; Zhu, X.X.; Garon, M.; Buschmann, M,D.; *Polymer*, **2004**, *45*, 71. **DOI:** 10.1016/j.polymer.2003.10.075
10. Gauthier, M. A.; Luo, J.T.; Calvet, D.; Ni, C.; Zhu, X.X.; Garon, M. ; Buschmann, M. D.; *Polymer*, **2004**, *45*, 8201. **DOI:** 10.1016/j.polymer.2004.09.055
11. Lee, J.; Joo, M.K.; Kim, J.; Park, J. S.; Yoon, M.Y.; Jeong, B.; *J. Biomater. Sci. Polym. Ed.*, **2009**, *20*, 957. **DOI:** 10.1163/156856209X444367
12. Klempner, D.; Frisch, K. C. (Eds.); Advances in InterpenetratingPolymer Networks; Technomic : USA, **1990**.
13. Frisch, K.C.;Wasserman, E.; *J. Am. Chem. Soc.*,**1961**, *83*, 3789. **DOI:** 10.1021/ja01479a015
14. Ajayan, P.M.; Schadler, L.S.;Giannaris, C.; *Adv. Mater.*,**2000**, *12*, 750. **DOI:** 10.1002/(SICI)1521
15. Qin, S.; Qin, D.; Ford, W.T.; Zhang, Y.;Kotov, N.A.; *Chem. Matr.*,**2005**,*17*, 2131. **DOI:** 10.1021/cm048239s
16. Ham, H.T.; Choi, Y.S.; Jeong, N.; Chung, I.J.; *Polymer*, 2005, *46*, 6308.

DOI: 10.1016/j.polymer.2005.05.062
17. Liu, L.; Barber, A.H.;Nuriel, S.; Wagner, H.D.; *Adv. Funct. Mater.*,**2005**, *15*, 975.
DOI: 10.1002/adfm.200400525
18. Bhattacharyya, A.R.;Potschke, P.; Abdel- Goad, M.; Fischer, D.; *Chem. Phys. Lett.*, **2004**, *392*, 28.
DOI: 10.1016/j.cplett.2004.05.045
19. Yihong, H.; Qingchun, F.; Chaobo, X.; *J. Appl. Polym. Sci.*, **2007**,*104*, 4068.
DOI: 10.1002/app.25686
20. Shanjun, G.;Lina, Z.; *J. Appl. Sci.*,**2001**,81, 2076.
DOI: 10.1002/app.1641
21. Constantina, S.;Panagiotis, K.;Stefanos, K.; Vladimir, G.;Polycarpos, P.;Lyudmyla, K.; *J. Polym. Sci. Part B: Polym. Phys.*, **2014**, *52*, 397.
DOI: 10.1002/polb.23427
22. Xiaoxia, J.; Legin, X.; Weiliang, Z.; Haiqin, D.; *Adv. Mater. Res.*, **2013**, *627*, 873.
DOI: 10.4028/www.scientific.net/AMR.627.873
23. Md.SelimArifSher, S.; Pratyay, B.; Sunkara, V.M.; *J. Phys. Chem.C.*, **2010**, *114*, 14281.
DOI: 10.1021/jp105450q
24. Lyudmyla, V.K.; Gisele, B.; Gerard, S.; Isabelle, S.; Andrew, W.L.; Sergey, V.M.;Mikle, H.;Lyudmyla, M.S.; Elena, D.L.; Anna, S.; *Polym. Eng. Sci.*,**2008**, *48*, 588.
DOI: 10.1002/pen.20965
25. Lyudmyla, V.K.; Sergey, V.M.; Andrew, W.L.; *J. Mater. Chem.*, **2012**, *22*, 7919.
DOI: 10.1039/C2JM16176A
26. Sen, R.; Zhao, B.; Perea, D.; Itkis, M. E. ; Hu, H.; Love, J.; Bekyarova, E.; Haddon, R. C.; Nano Lett., **2004**, *4*, 459.
DOI: 10.1021/nl035135s
27. Karabanova, L. V.;Sergeeva, L.M.;Svyatyna, A.V.;Yakushev, P. N.;Egorova, L. M.;Ryzhov, V. A.;Bershtein, V.A.; *J. Polym. Sci. Part B: Polym. Phys.*, **2007**, *45*, 963.
DOI: 10.1002/polb.21108
28. Hui, H.; Ni, Y.C.;Mandal, S.K.; Montana, V.; Zhao, B.; Haddon, R.C.;Parpura, V.; *J. Phys. Chem. B.*, **2005**, *109*, 4285.
DOI: 10.1021/jp0441137
29. Sen, R.; Zhao, B.;Perea, D.;Itkis, M.E.; Hu, H.; Love, J.; *Nano Lett.*,**2004**, *4*, 459.
DOI: 10.1021/nl035135s
30. Jaisankar, S. N.; Nelson, D. J.; Ravi Kumar, D. J.;Mandal, A. B.; *AIChE.*, **2014**, *60*, 820.
DOI: 10.1002/aic.14336
31. Ma, Z.; Gao, J.; Huai, Y.; Guo, J.; Deng, Z.; Suo, J.; *J. Sol- Gel Sci. Technol.*,**2008**, *48*, 267.
DOI: 10.1007/s10971-008-1813-1
32. Breuer, O.; Sundararaj, U.; *Polym. Comp.*, **2004**, *25*, 630.
DOI: 10.1002/pc.20058
33. Xie, X. L.; Mai, Y. W.; Zhou, X. P.; *Mater. Sci. Eng. Res.*, **2005**, *49*, 89.
DOI: 10.1016/j.mser.2005.04.002
34. Moniruzzaman, M.; Winey, K. I.; *Macromolecules*,**2006**, *39*, 5194.
DOI: 10.1021/ma060733p
35. Fiedler, B.; Gojny, F. H.; *Compos. Sci. Technol.*, **2006**, *66*, 3115.
DOI: 10.1016/j.compscitech.2005.01.014
36. Gibson, R. F.; Ayorinde, E. O.; Wen, Y. F.; *Compos. Sci. Technol.*, **2007**, *67*, 1.
DOI: 10.1016/j.compscitech.2006.03.031
37. Bal, S.; Samal, S.; *Bull. Mater. Sci.*, **2007**, *30*, 379.
38. Samanta, D.; Murali Sankar, R.; Jaisankar, S. N.; SayemAlamb, M. D.; Mandal, A. B.; *Chem Commun.*,**2011**, *47*,11975.
DOI: 10.1039/c1cc14818d
39. (i) Mandal, S. K.; Kar, T. D.; Das, P. K.; *Chem.Commun.*, **2012**, *48*,1814.
(ii) Samanta, S. K.; Pal, A.; Bhattacharya, S.; Rao, C. N. R.; *J. Mater. Sci.*, **2010**, *20*, 6881.
DOI: (i)10.1039/C2CC16567H
(ii)10.1039/c0jm00491j
40. Nelson, D. J.; Perumal, P. T.; Brammer, C. N.; Selvam, N. P.; *J.Phys.Chem.C.*,**2009**, *113*, 17378.
DOI: 10.1021/jp9072075
41. Gangoli, V. S.; Azhang, J.; Willett, T.T.; Gelwick, S. A.; Haroz, E. H.; Kono, J.; Hauge, R. H.; Wong, M. S.; *Nanomater. Nanotechnol.*, **2009**, *4*, 19.
DOI: 10.5772/58828
42. Muralisankar, R.; Seeni Meera, K.; Mandal, A. B.; Jaisankar, S. N.; *High perform. Polym.*, **2012**, *25*, 135.
DOI: 10.1177/0954008312459545
43. Ungur, G.; Hruza, J; *Adv. Mat. Lett.*, 2014, *5*, 422.
DOI: 10.5185/amlett.2014.amwc1025
44. Shivakumar Gouda, P.S.; Kulkarni, R.; Kurbet, S.N.; Jawali, D.; *Adv. Mat. Lett.*, 2013, *4*, 261.
DOI: 10.5185/amlett.2012.9419
45. Turhan, Y.; Dogan, M.; Alkan, M.; *Ind. Eng.Chem. Res.*, **2010**, *49*, 1503.
DOI: 10.1021/ie901384x
46. Dong, Q. X.; Chen, Q. J.; Yang, W.; Zheng, Y. L.; Liu, X.; Li, Y. L.; Yang, M. B.; *J. Appl. Polym. Sci.*, **2008**, *109*, 659.
DOI: 10.1002/app.28053
47. Marshall a, M. W.; Popa-Nita b, S.; Shapter a, J. G.; *Carbon*, **2006**, *44*, 1137.
DOI: 10.1016/j.carbon.2005.11.010
48. Borach, D.; Ghoshal, T.; Shaw, M. T.; Chaudhari, A.; Petkov, N.; Bell, A. P.; Holmes, J. D.; Morris, M. A.; *Nanomater. Nanotechnol.*, **2014**, *4*, 25.
DOI: 10.5772/59098

Supporting Information

ESI Table 1. The sample code and compositions of PU nanotube composites.

Sample code	IPDI (g)	PEG (g)	PVA (g)	TMP (g)	*f-SWCNTs* (Wt %)
PU					-
PUNT1					0.001
PUNT2	2	1	2	0.166	0.005
PUNT3					0.010
PUNT4					0.050
PUNT5					0.100

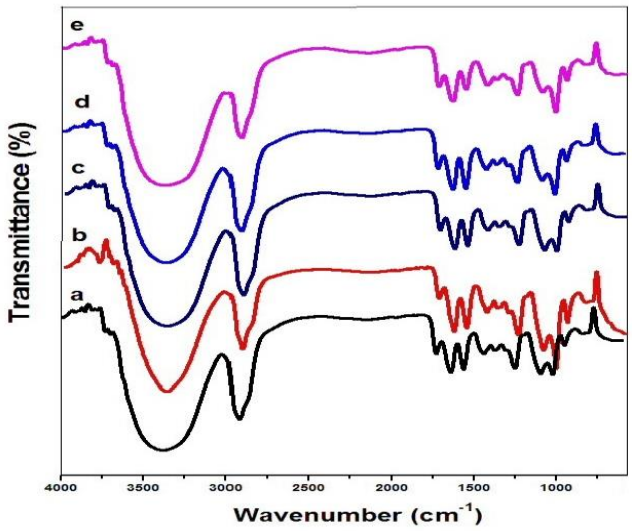

ESI Fig. 1. ATR-IR spectra of (a) PVA, (b) PU (c) PUNT1 (d) PUNT3 and (e) PUNT5.

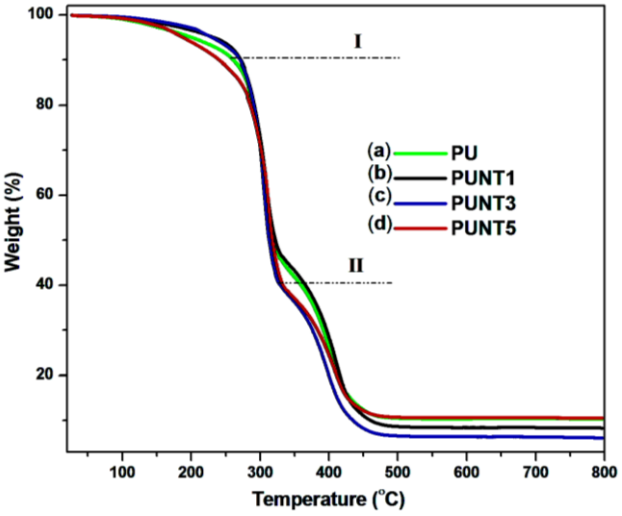

ESI Fig. 2. A TG curves of: (a) PU, (b) PUNT1, (c) PUNT3 and (d) PUNT5.

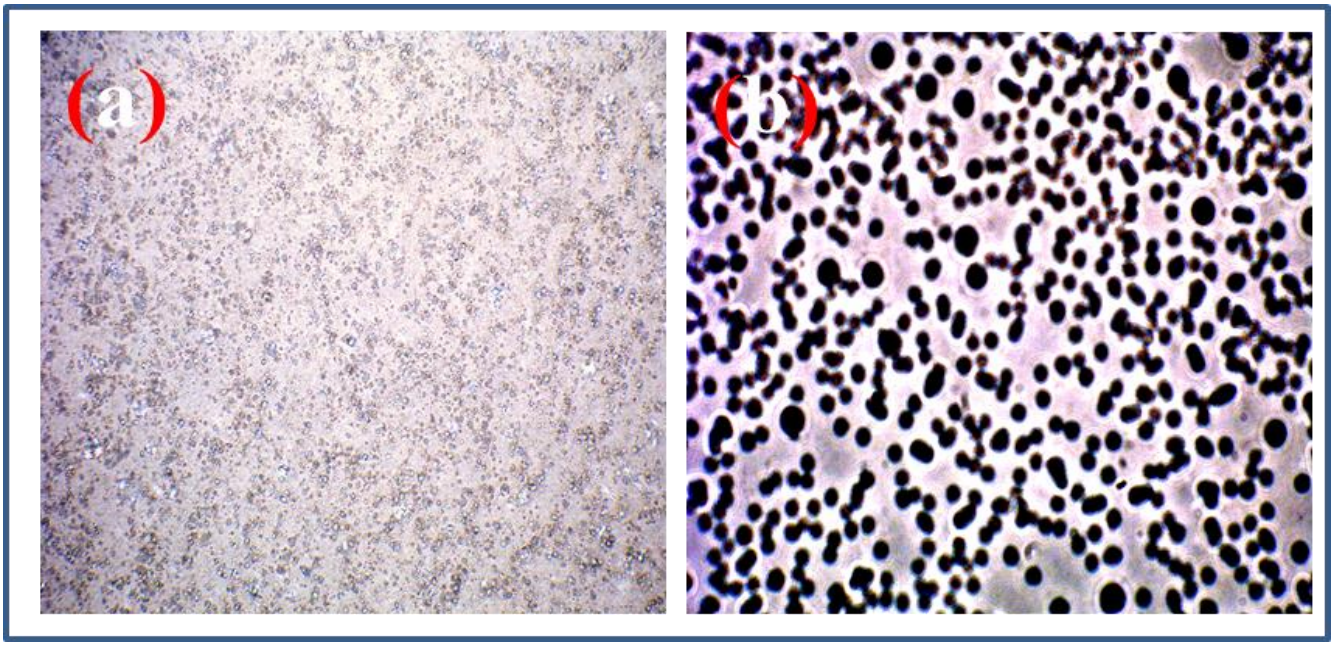

ESI Fig. 3. Morphology of semi-IPNsbased OPM (a) PU and (b) PUNT5.